obtain Eq. 5, we take the magnitude squared of the sum of the fields for two identical beams in phase or 180° out of phase, $\psi(\mathbf{x} - \mathbf{x}_0,z)\exp(i\mathbf{u}\cdot\mathbf{x} + i\phi) \pm \psi(\mathbf{x} + \mathbf{x}_0,z)\exp(-i\mathbf{u}\cdot\mathbf{x} + i\phi)$, multiplied by a normalizing constant to set the total power to P. The relative phase is $\theta = -2\mathbf{u}\cdot\mathbf{x}$, where $\mathbf{u} = -kn_0\, q\mathbf{x}(0)\sin(q,z)$.

18. For a given power, the trajectory is independent of phase, unlike in a local nonlinearity [L. Poladian, A. W. Snyder, D. J. Mitchell, *Opt. Commun.* **85**, 59 (1991)].
19. The parabolic medium induced by the two beams depends on their total power $P_c - \delta$ through the coefficient $\alpha(P)$ in Eq. 1, so $\alpha \cong \alpha(P_c)$. The axis of this parabolic medium is determined by the first moment of the composite two-beam intensity distribution as discussed below Eq. 2. It is thus centered approximately on the bright beam. Propagation then follows from the physics of the parabolic medium (*14, 15*). The dim beam is displaced from the axis and so undergoes sinusoidal oscillations about the bright beam, whereas the on-axis bright beam travels straight. Further, the dim and bright beam have the same width—that necessary to remain uniform in the $\alpha \cong \alpha(P_c)$ parabolic medium.
20. Y. Silberberg, *Opt. News* **15**, 7 (1989).
21. We previously (*22, 23*) showed that linear physics provides deep insight into the soliton dynamics of a local nonlinear medium, but large nonlocality allows us to demonstrate the concept with particular elegance and to obtain exact closed-form expressions for collisions.
22. A. W. Snyder, D. J. Mitchell, Y. S. Kivshar, *Mod. Phys. Lett. B* **9**, 1479 (1995).
23. A. W. Snyder, *Opt. Photonics News* **7**, 17 (1996); ______ and D. J. Mitchell, *Opt. Lett.* **22**, 16 (1997); A. W. Snyder, S. J. Hewlett, D. J. Mitchell, *Phys. Rev. Lett.* **72**, 1012 (1994).

24. We thank N. Akhmediev, P. Chiao, Y. Kivshar, F. Ladouceur, M. Segev, and R. Shen for insight. The authors are part of the Australian Photonics Cooperative Research Centre.

13 January 1997; accepted 14 April 1997

Preservation of Chitin in 25-Million-Year-Old Fossils

B. Artur Stankiewicz, Derek E. G. Briggs, Richard P. Evershed, Matthew B. Flannery, Michael Wuttke

Chitin is present in fossil insects from the Oligocene (24.7 million years ago) lacustrine shales of Enspel, Germany. This result, which was obtained by analytical pyrolysis, extends by nearly 25 million years the length of time that chemically detectable remains of this biomolecule are known to survive. The embedding sediment is dominated by diatoms, which reflect high productivity in the paleolake. The primary control on the preservation of chitin is thus not time; it may persist in older sediments where suitable paleoenvironmental conditions prevailed.

Chitin, which is one of the most abundant macromolecules on Earth, is also one of the most enigmatic of molecular fossils. An estimated 10^{11} tons of chitin is produced annually in the biosphere, most of it in the oceans (*1*). It occurs in a range of organisms but is particularly important as a constituent of arthropod cuticles (*1–4*), where it is cross-linked with proteins via catechol and histidyl moieties (*5*). Although biodegradation in the water column and sediment normally removes almost all of the chitin produced in the oceans (*3*), experiments have demonstrated that chitin is the component of shrimps that is most resistant to degradation (*6*) and organic remains of arthropod cuticle are abundant in the fossil record, in some cases preserving remarkable morphological detail (*7*). Chitin has been detected in insects in terrestrial deposits of Pleistocene age (~130,000 years ago) (*8*) and in asphalt deposits from California (*9*). However, analyses have failed to provide evidence for its presence in older fossils except (*6, 10–12*) for traces of amino sugars in the calcified skeletons of one Cretaceous and three Tertiary decapod crustaceans (*13*). Even where the morphology of the cuticle appears well preserved, the original chemical composition may be completely altered.

Pyrolysis–gas chromatography–mass spectrometry (py-GC-MS) (*6, 14–16*) provides a powerful tool for the chemical characterization of invertebrate cuticles (*9, 15*), particularly in cases in which the sample size is limited to a few micrograms. Investigation of the cuticles of fossil arthropods from 15 sites ranging in age from Silurian to Cretaceous revealed no trace of the original chemical components of chitin (*12*). The chemical signature either (i) was dominated by the *n*-alk-1-ene and *n*-alkane doublets characteristic of highly aliphatic biopolymers or (ii) contained a substantial aromatic component including alkylbenzenes and alkylindenes and relatively abundant sulfur-containing compounds such as thiophenes (*12*).

Here we demonstrate that chitin is preserved in the late Oligocene [24.7 million years ago (Ma)] Enspel Fossillagerstätte (*17*) near Bad Marienberg, in the Westerwald, Rheinland-Pfalz, Germany, where maar-lake deposits are interbedded with tuff

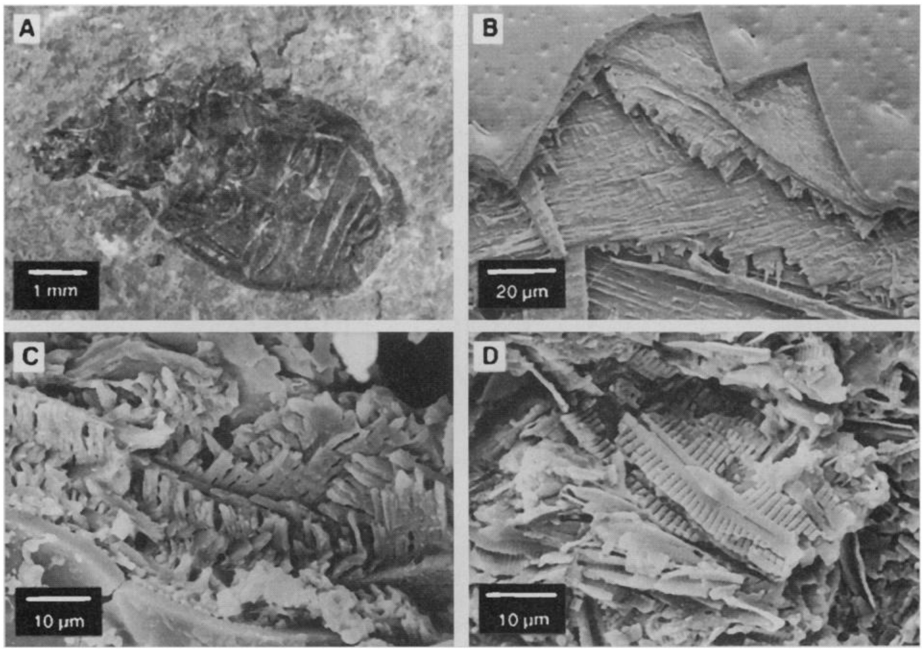

Fig. 1. Photomicrographs of (**A**) the ventral view of a beetle (Coleoptera: Curculionoidea) from level 12 of the Oligocene (24.7 Ma) of Enspel, western Germany; (**B**) an SEM image of the cuticle of a modern mealworm beetle (*Tenebrio molitor*) that reveals the layers of cuticle overlapping at different angles; (**C** an SEM image of a fractured edge of cuticle of the specimen illustrated in (A) that shows chitinous fibers; and **D**) an SEM image of the shale matrix that contains the fossil insects and reveals that pennate diatoms are the dominant constituent. (Images were made with a Cambridge Stereoscan 250 Mk3 SEM at 7 to 12 kV after specimens were coated with gold.)

B. A. Stankiewicz and D. E. G. Briggs, Biogeochemistry Research Centre, Department of Geology, University of Bristol, Queen's Road, Bristol BS8 1RJ, UK.
R. P. Evershed and M. B. Flannery, Organic Geochemistry Unit, School of Chemistry, University of Bristol, Cantock's Close, Bristol BS8 1TS, UK.
M. Wuttke, Landesamt für Denkmalpflege Rheinland-Pfalz, Referat Erdgeschichtliche Denkmalpflege, Am Obstmarkt 13, D-55126 Mainz, Germany.

(*18*). This deposit yields abundant remarkably preserved plants and animals (*18*), complete with soft body outline, and insects, some of which retain the original iridescent color. We used py-GC-MS (*19*) to study beetles [eight specimens of Coleoptera: Curculionoidea (Fig. 1A)] and flies (two specimens of Diptera: Bibionidae), which represent the dominant insect orders from Enspel (*20*), from the 14-cm-thick layer 12 in the bituminous volcanoclastic shales (*21*).

The distribution of major pyrolysis products of the Enspel beetles is similar to that in elytra of modern beetles (Fig. 2, A and B). The prominent pyrolysis products of chitin, including acetamide, *N*-acetyl-2-pyridone, acetamidofuran, 3-methyl-5-acetamidofuran, 3-acetamido-4-pyrone, oxazoline derivatives, acetic acid, and pyridines, are present in the fossil samples. Although the distribution of certain components varies among samples, the pyrograms of all the beetle cuticles reveal a similar pattern (Fig. 2). The same diagnostic components are evident in the pyrolysate of chitin isolated from modern arthropods (*15*). Analyses of the Enspel flies, however, revealed that none of the pyrolysis products were directly related to chitin but instead they composed a series of *n*-alk-1-enes and *n*-alkanes characteristic of older fossil arthropod cuticles that have been diagenetically altered (*12*).

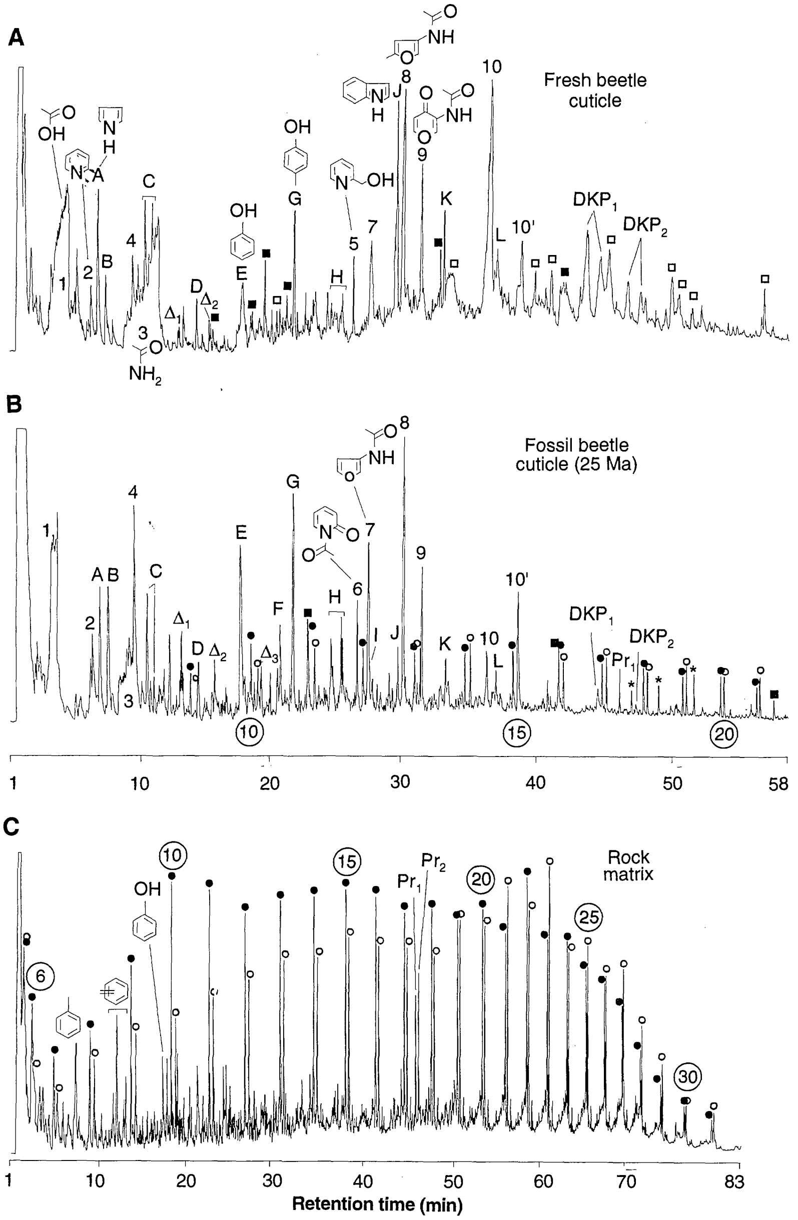

Fig. 2. Total ion chromatograms (pyrolysis at 610°C for 10 s) of the (**A**) elytra of a modern mealworm beetle (*Tenebrio molitor*), (**B**) cuticle of the curculionoid beetle from Enspel, and (**C**) sedimentary matrix from Enspel level 12. The numbers indicate major pyrolysis products derived from chitin: 1, acetic acid; 2, pyridine; 3, acetamide; 4, methylpyridine; 5, 2-pyridinemethanol; 6, *N*-acetyl-2-pyridone; 7, 3-acetamidofuran; 8, 3-acetamido-5-methylfuran; 9, 3-acetamido-4-pyrone; and 10, 10 and 10′-oxazoline derivatives. Solid squares indicate important components directly related to chitin polymer. Letters indicate products derived from amino acids: A, pyrrole; B, toluene; C, methylpyrroles; D, ethylpyrrole; E, phenol; F, 2-methylphenol; G, 4-methylphenol; H, dimethylphenol and ethylphenol; I, vinylphenol; J, indole; K, methylindole; L, dimethylindole; DKP$_1$, 2,5-diketopiperazine of pro-Ala; and DKP$_2$, 2,5-diketopiperazine of pro-Val. Open squares indicate other important components related to proteins. Δ_{1-3}, cyclic ketones derived from carbohydrate moieties; solid circles, *n*-alk-1-enes; open circles, *n*-alkanes; Pr$_1$, prist-1-ene; Pr$_2$, prist-2-ene; asterisks, contamination. Circled numbers indicate the carbon number in the aliphatic chains. Chemical structures are given for most of the important pyrolysis products.

Pyrolysis of the shale matrix that contains the Enspel fossils (Fig. 2C) produced a series of C_5 to C_{31} *n*-alk-1-enes, *n*-alkanes, and α,ω-alkadienes. This trace is characteristic of highly aliphatic resistant macromolecules such as algaenan (derived from algae) and cutan [from the cuticle of vascular plants (*22*)], both of which are major contributors to Type I kerogens. This pyrolysis trace differs from that of the cuticle of the Enspel flies in that abundant C_{20} to C_{34} alkene/alkane pairs are present (Fig. 2C). Scanning electron microscopy (SEM) reveals that the matrix consists overwhelmingly of pennate diatoms (Fig. 1D), although the presence of other algae has been reported (*23*). Thus, there are a number of possible sources of the highly aliphatic signature of the sedimentary matrix. Such a series of *n*-alk-1-enes and *n*-alkanes is also evident among the pyrolysis products of fossils to which the matrix adhered and from which it could not be completely removed (Fig. 2B).

The presence of 2,5-diketopiperazines, which are diagnostic pyrolysis products of proteins (*15, 24*), indicates that a protein component has survived in the beetle cuticle in addition to the chitin macromolecule. A number of other pyrolysis products are also derived from amino acids, such as tyrosine (phenol and methylphenols), tryptophan (indole and methylindole), phenylalanine (toluene) and proline (pyrrole and methylpyrroles) (Fig. 2A). Although protein moieties have been shown to be more susceptible to decay than chitin in laboratory experiments (*6*), they appear to be important components of the Enspel fossil samples. The presence of 2-cyclopenten-1-ones, the products of carbohydrate moieties, provides further evidence of the chemical preservation of the beetle cuticle.

SEM of the fossil beetle cuticles from Enspel revealed the overlapping layers of thick fibers in the cuticle (Fig. 1C). The appearance of the curculionid cuticle from Enspel is similar to that of modern beetles (Fig. 1B), although the organic matrix surrounding the fibers has partially degraded. The preservation of chitin in the beetles and not in the flies may reflect the greater thickness and degree of cross-linking in the cuticle of the former. This study demonstrates that the primary control on the preservation of these biomolecules in ancient rocks is not time but the nature of the depositional environment and the inhibition of diagenetic alteration. In the case of Enspel, the combination of high productivity (evidenced by the abundance of diatoms in the matrix) and strongly reducing bottom conditions (*23*) played a key role in the enhanced preservation of the chitin-protein complex.

REFERENCES AND NOTES

1. G. W. Gooday, *Adv. Microb. Ecol.* **11**, 387 (1990).
2. R. A. A. Muzzarelli, in *Chitin* (Pergamon, Oxford, 1977), pp. 5–155; A. Schimmelmann and M. J. DeNiro, *Geochim. Cosmochim. Acta* **50**, 1485 (1986).
3. M. Poulicek and C. Jeuniaux, *Biochem. Syst. Ecol.* **19**, 385 (1991).
4. K. J. Kramer, T. L. Hopkins, J. Schaefer, *Insect Biochem. Mol. Biol.* **25**, 1067 (1995).
5. J. Schaefer *et al.*, *Science* **235**, 1200 (1987).
6. M. Baas, D. E. G. Briggs, J. D. H. van Heemst, A. Kear, J. W. de Leeuw, *Geochim. Cosmochim. Acta* **59**, 945 (1995).
7. D. E. G. Briggs and E. N. K. Clarkson, *Trans. R. Soc. Edinb. Earth Sci.* **890**, 293 (1989); N. J. Butterfield, *Nature* **369**, 477 (1994).
8. R. F. Miller, M.-F. Voss-Foucart, C. Toussaint, C. Jeuniaux, *Palaeogeogr. Palaeoclimatol. Palaeoecol.* **103**, 133 (1993).
9. B. A. Stankiewicz, D. E. G. Briggs, R. P. Evershed, I. J. Duncan, *Geochim. Cosmochim. Acta*, in press.
10. M.-F. Voss-Foucart and C. Jeuniaux, *J. Paleontol.* **46**, 769 (1972).
11. A. Schimmelmann, R. G. F. Krause, M. J. DeNiro, *Org. Geochem.* **12**, 1 (1988).
12. B. A. Stankiewicz, D. E. G. Briggs, R. P. Evershed, *Energy Fuels*, in press.
13. D. Brumioul and M. F. Voss-Foucart, *Comp. Biochem. Physiol.* **57B**, 171 (1977).
14. R. A. Franich, S. J. Goodin, A. L. Wilkins, *J. Anal. Appl. Pyrolysis* **7**, 91 (1984); A. van der Kaaden *et al.*, *Anal. Chem.* **56**, 2160 (1984).
15. B. A. Stankiewicz *et al.*, *Rapid Commun. Mass Spectrom.* **10**, 1747 (1996).
16. P. F. van Bergen *et al.*, *Acta Bot. Neerl.* **44**, 319 (1995).
17. F. Schlunegger, D. W. Burbank, A. Matter, B. Engesser, C. Mödden, *Eclogae Geol. Helv.* **89**, 753 (1996).
18. G. Storch, B. Engesser, M. Wuttke, *Nature* **379**, 439 (1996).
19. The specimens were isolated from the sediment matrix mechanically and were extracted in CH_2Cl_2 before pyrolysis to eliminate contaminants. A quantity of each sample (0.05 to 0.005 mg) was pyrolyzed in a flow of helium for 10 s in a platinum coil at 610°C with the use of a Chemical Data System (Oxford, PA) 1000 Pyroprobe coupled to a Carlo Erba (Milan, Italy) 4130 gas chromatograph (GC) with a Finnigan (Sunnyvale, CA) 4500 mass spectrometer (MS). Compounds were separated with a Chrompack (Middelburg, Netherlands) 50-m CP Sil-5 column (0.32-mm inside diameter and film thickness of 0.4 μm). The GC oven was operated as follows: isothermal at a temperature of 35°C for 5 min, with temperature programmed at 4°C per minute to 310°C, and then again at the isothermal temperature for 10 min. The MS was operated in full scan mode (35 to 650 daltons, 1 scan per second, 70 eV of electron energy). Peaks were identified on the basis of their mass spectral characteristics and GC retention indices; by comparison with authentic chitin, protein, and amino acid standards (*15*); and with reference to the literature (*14*).
20. S. Wedmann and G. Tröster, *Cour. Forschungsinst. Senckenb.*, in press.
21. G. Radtke and M. Wuttke, *ibid.*, in press.
22. E. W. Tegelaar, J. W. de Leeuw, S. Derenne, C. Largeau, *Geochim. Cosmochim. Acta* **53**, 3103 (1989).
23. L. Schwark, M. Giessen, B. Spitthoff, D. Leythaeuser, *Cour. Forschungsinst. Senckenb.*, in press.
24. M. A. Ratcliff Jr., E. E. Medley, P. G. Simmonds, *J. Org. Chem.* **39**, 1482 (1974).

25. J. Carter and A. Gledhill (mass spectrometry facilities), S. Kearns (SEM), S. Powell (photography), and I. Duncan (modern insects) provided essential support, and we benefited from discussions with P. van Bergen and H. Poinar. M. Poschmann assisted with the collection of the samples. S. Wedmann identified the fossil insects. Supported by the Natural Environmental Research Council (NERC) grant GST/02/1027 to D.E.G.B. and R.P.E.; NERC also supported mass spectrometry facilities (grants GR3/2951 and GR3/3758). Collaboration between D.E.G.B. and M.W. was funded by the British-German Academic Research Collaboration program.

21 February 1997; accepted 16 April 1997

A Nestling Bird from the Lower Cretaceous of Spain: Implications for Avian Skull and Neck Evolution

José L. Sanz, Luis M. Chiappe, Bernardino P. Pérez-Moreno,
José J. Moratalla, Francisco Hernández-Carrasquilla,
Angela D. Buscalioni, Francisco Ortega,
Francisco J. Poyato-Ariza, Diego Rasskin-Gutman,
Xavier Martínez-Delclòs

A feathered skeleton of a Lower Cretaceous enantiornithine bird from Spain indicates that the modified diapsid skull of modern birds did not evolve until late in their evolution: Basal birds retained an essentially primitive diapsid design. The fossil provides data clarifying long-standing debates on the cranial morphology of the basalmost bird, *Archaeopteryx*. It also reemphasizes the notion that the early morphological transformations of birds were focused on the flight apparatus. This fossil was a nestling and suggests that early postnatal developments in the Cretaceous enantiornithine birds and those in their extant counterparts are comparable.

In recent years, a profusion of Mesozoic avians has greatly augmented existing knowledge on the early phases of bird evolution. These findings document an enormous diversity of basal birds and provide the foundations for a more accurate reconstruction of the morphological changes leading to the modern avian design (*1–3*). However, these important data have not advanced our understanding of early transformations of the avian skull and neck much beyond what was learned from the first complete skull of *Archaeopteryx* unearthed over 100 years ago.

Here we describe a fossil bird from the Lower Cretaceous La Pedrera Konservat-Lagerstätte, a renowned locality of the La Pedrera de Rúbies Lithographic Limestones Formation in the Spanish Serra de El Montsec (south-central Pyrenees, in the province of Lleida) (*4*). Its skull (*5*) (Figs. 1 and 2) is slightly crushed: the right side is elevated and displaced forward (Fig. 3). The first 12 presacral vertebrae are preserved, along with parts of both wings and shoulders, part of the sternum, and some incomplete feathers. Large clusters of tiny foramina interrupt the periosteal bone of the cervical vertebrae, humerus, ulna, and the articular region of the mandible, a pattern of ossification found in neonates of modern birds (Fig. 4). The incomplete ossification of the periosteal bone and the relative proportions of (i) the orbit and the rostrum and (ii) the skull and the postcranium strongly suggest that the bird was immature, most likely a nestling (*6*).

The toothed skull is similar to that of *Archaeopteryx* (*7–9*). It is subtriangular, with a large circular orbit and a vaulted braincase (Fig. 3). The snout is roughly half the total length of the skull. The external nares are subelliptical and slightly larger than the triangular antorbital fossa.

As in *Archaeopteryx* (*7–9*) and in the

J. L. Sanz, B. P. Pérez-Moreno, J. J. Moratalla, A. D. Buscalioni, F. Ortega, F. J. Poyato-Ariza, Unidad de Paleontología, Departamento de Biología, Facultad de Ciencias, Universidad Autónoma de Madrid, 28049 Madrid, Spain.
L. M. Chiappe, Department of Ornithology, American Museum of Natural History, New York, NY 10024, USA.
F. Hernández-Carrasquilla, Unidad de Arqueozoología, Departamento de Biología, Facultad de Ciencias, Universidad Autónoma de Madrid, 28049 Madrid, Spain.
D. Rasskin-Gutman, Department of Paleobiology, MRC 121, National Museum of Natural History, Smithsonian Institution, Washington, DC 20560, USA.
X. Martínez-Delclòs, Departament de Geologia dinàmica, Geofísica i Paleontologia, Facultat de Geologia, Universitat de Barcelona, 0871 Barcelona, Spain.